



OPEN

# Comparative analysis of adding cotton straw and corn stover to improve the combustion performance of municipal sludge

Feng Xu<sup>1,2</sup>, Jing Li<sup>1✉</sup> & Zihan He<sup>1</sup>

To address issues of high water content and low calorific value during combustion of municipal sludge, we added water-absorbent, easy-to-burn agricultural waste to improve the overall combustion performance. Cotton straw or corn stover were added to the sludge and mixed at high-speed to compare their capacities for improving combustion performance. Scanning Electron Microscopy (SEM) revealed that cotton straw or corn stover attached to the surface of the municipal sludge particles after blending, while analysis of thermogravimetric curves and activation energies of the blends showed that combustion and exhaustion rates increased significantly when 40% cotton straw or corn stover were blended into the sludge. Using the quadrilateral cut-ring boiler as a prototype, the mix of sludge with cotton straw or corn stover was simulated, and FLUENT software was used to obtain the temperature and pollutant emissions of the boiler. Sludge blended with cotton straw or corn stover increased furnace temperature and reduced SO<sub>2</sub> and NO emissions, while that with cotton straw burned at higher temperatures with lower SO<sub>2</sub> and NO emissions. Overall, the CO content of sludge combustion was lower when blended with proportions of cotton straw or corn stover under 50%. The findings of this study lay a theoretical foundation for treatment of municipal sludge according to local conditions.

Various industries have developed carbon reduction methods as part of the “dual carbon” goals in China. In the western region, thermal power plants are prioritizing energy conservation and environmental protection by achieving carbon and consumption reduction. Additionally, alternatives to traditional coal fuel have become a popular research topic. Municipal sludge, regarded as solid waste, is considered a type of “fuel”<sup>1</sup> due to its certain calorific value and required processing amount<sup>2</sup>. The “Urban Domestic Wastewater Treatment Facilities to Make Up for the Shortfall” covers waste treatment; specifically, the “Implementation Program of Mending Shortcomings and Strengthening Weaknesses of Urban Living Sewage Treatment Facilities”<sup>3</sup> states that “large and medium-sized cities in the central and western regions of China must reduce the scale of sludge landfills. In large and medium-sized cities where land resources are scarce, the use of ‘biomass utilization + incineration’ disposal mode is encouraged”.

Xinjiang is located in the northwestern border of China; thus, it acts as an important gateway connecting Central Asia and Europe and as an important node of the “One Belt, One Road” strategy. Its geographic location provides Xinjiang with a wide space and opportunities for development and cooperation; thus, Xinjiang is one of China’s major agricultural provinces and the largest producer of cotton<sup>4</sup>. However, agricultural waste in this region has a low utilisation rate<sup>5,6</sup>, necessitating investigation of the performance characteristics of waste for use in synergistic resource utilisation, sustainable waste treatment, and the establishment of a low-carbon, energy-efficient, and environmentally friendly municipal sludge processing strategy.

Researchers have attempted to co-combust municipal sludge and biomass to improve sludge combustion. For example, Yuanyuan et al.<sup>7</sup> (2022) reported that when 60% sludge was blended with 40% peanut shells, the combined combustion performance index increased by 6.9 times, the volatile release characteristic index increased by 4.5 times, and the activation energy decreased by 19.43 kJ/mol. Additionally, Geon-Uk Baek<sup>8</sup> et al. (2020) reported that reduction of SO<sub>2</sub>, NO and CO by 70.8, 77.1 and 38.2%, respectively, for 50%t sludge versus 50% woody biomass combustion. Wang<sup>9</sup> et al. (2020) investigated the combustion and emission characteristics of sludge mixed with biomass, such as rice husks, and concluded that the NO<sub>x</sub> and SO<sub>2</sub> emissions from 80%

<sup>1</sup>School of Civil Engineering and Architecture, Xinjiang University, Urumqu 830049, China. <sup>2</sup>Faculty of Environment, Harbin Institute of Technology, Harbin 15001, China. ✉email: lj1906348604@163.com

biomass + 20% sludge were lower than those from sludge combustion,  $\text{NO}_x$  was reduced by about 66% and  $\text{SO}_2$  by 80%. Further, Jingyong Liu<sup>10</sup> et al. (2018) concluded that 60.1% blending of sewage sludge and water hyacinth resulted in the best combustion parameters at a heating rate of 29.9 °C/min, and a maximum burnout rate of 92.4%. Jin-Ho Sung<sup>11</sup> et al. (2018) concluded that 70% sludge + 30% biomass, with 23% oxygen mixing rate. When burning in a 30 kWth CFB, lowest temperature gap between riser and stack occurred, high enrichment of  $\text{CO}_2$  (over 90%) with less pollutant emissions, specifically 0.91% CO and 14 ppm NO.

Given the large-scale production of urban sludge containing high moisture<sup>12</sup> content, low calorific value<sup>13,14</sup>, low level of resource utilization and low recycling of energy, as well as that of cotton straw and corn stover (containing high cellulose and hemicellulose contents and calorific value)<sup>15–17</sup>, in Xinjiang, this study features a comparative analysis on the combustion performance of urban sludge after addition of different proportions of cotton straw or corn stover waste. Using the advantages of Computational Fluid Dynamics (CFD), such as high operability, low cost, and effective observation of the combustion process<sup>18</sup>, the temperature and flue gas distribution of sludge mixed with cotton straw (or corn stover) in a quadrangular cut-circle boiler were solved by Fluent software. Studies of this nature are critical in the search for new biomass fuels to replace fossil fuels in thermal power plants, and for providing theoretical support for cleaner production while synergistically promoting carbon and pollution reduction. A schematic diagram of the synergistic resource utilisation strategy for treatment of municipal sludge is shown in Fig. 1.

## Materials and methods

### Materials and pre-processing

The experimental sludge was obtained from the domestic wastewater treatment plant (WWTP) ex-factory sludge with 80% water content. The wastewater treatment process of this wastewater treatment plant is activated sludge method. The effluent sludge is the sludge after dosing, disinfection and mechanical dewatering and is disinfected. The experimental mud is not dried above 60 °C. The sludge is a zoogloea and there is no bacteria treatment during the whole process. The cotton straw used in the experiment were obtained from cotton straw of long-staple cotton harvested in autumn in Xinjiang. The corn stover used in the experiment came from the corn stover of MC670 corn after harvesting in autumn in Xinjiang. Natural air drying of sludge taken from sewage treatment plant, and then subject to the use of RRH-100 crusher, take 0.075 mm sludge particles for spare. Cotton straw, and corn stover were pre-processed the same way, the same RRH-100 crusher was used to crush and 0.075 mm particles were taken for spare.

### Experimental methods

#### Mixing methods

An RRH-100 crusher, set at a mixing speed of 28,000 rpm, was used as the mixing device. Figure 2 shows a schematic diagram of the blending process. Sludge with a particle size of 0.075 mm was placed in a mixing unit with cotton straw (or corn stover) and stirred for 5 min. The mixing device oscillated at a uniform speed during the mixing process, which promoted the homogeneous mixing of the sludge with the cotton straw or corn stover.

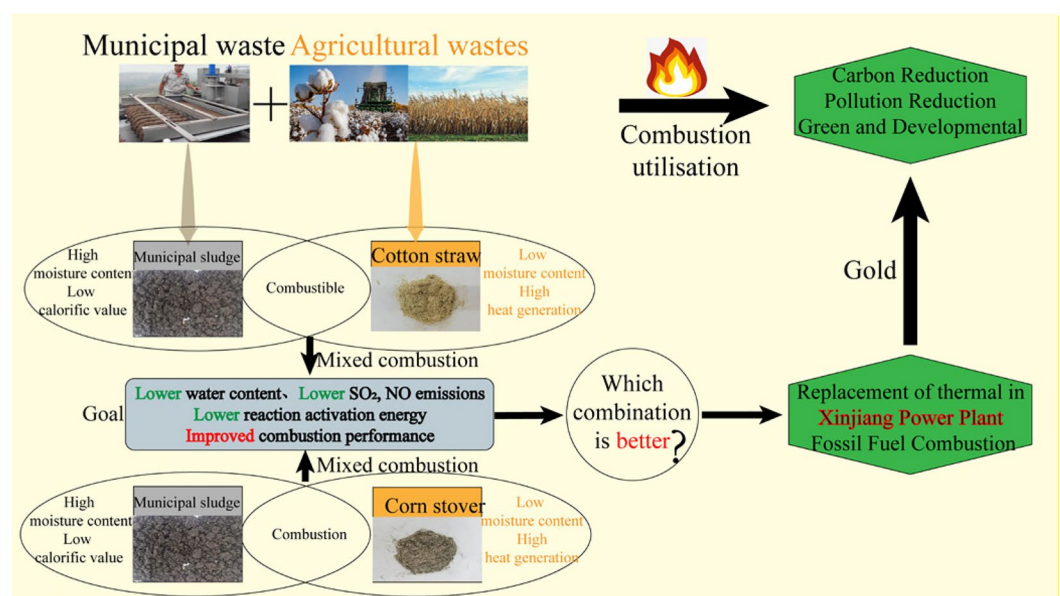


**Figure 1.** Conceptualization of municipal Sludge Combustion in Xinjiang.

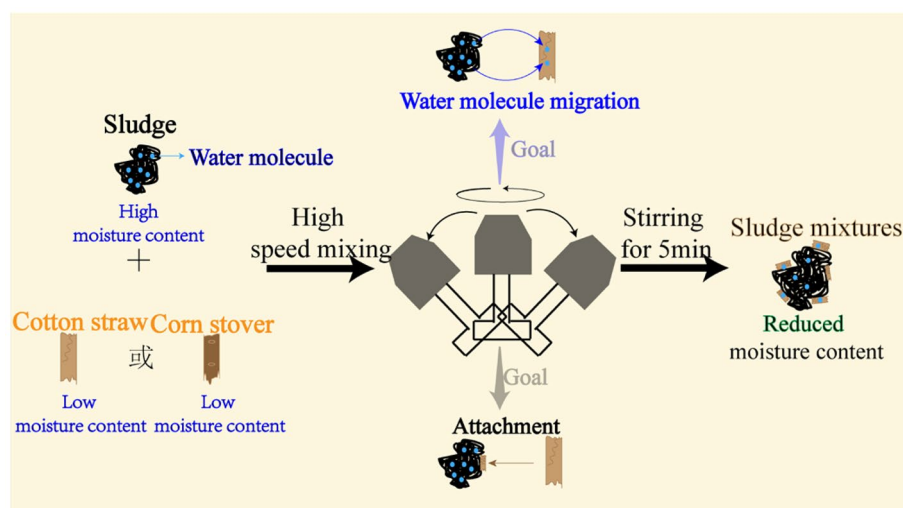


**Figure 2.** Schematic diagram of the method for blending sludge with cotton straw or corn stover.

#### *Elemental and industrial analyses and calorific value*

The elemental contents of C, H, O, and N, as well as moisture, ash, volatile matter, fixed carbon content, and calorific value of the sludge, cotton straw, and corn stover were measured in accordance with The Elemental Analysis of Coal (GBT31391-2015), The Industrial Analysis of Coal (GBT212-2008), and Determination of the Coal Heat Generation Method (GBT213-2008). Table 1 shows the instrument types and models.

#### *Microstructure analysis*

Scanning electron microscopy was carried out using a German Zeiss SEM field emission scanning electron microscope GeminiSEM 300 for microstructure observation. A 10 mg substrate, with a particle size of 0.075 mm, was glued to the conductive adhesive, then 45 s gold spraying with 10 mA using a Quorum SC7620 sputter coater. Working distance is 8.5 mm. The acceleration voltage was set to 3 kV and a magnification of 2000X for morphology filming. The microstructures of sludge, cotton straw, and corn stover were observed and analysed before and after blending.

#### *Thermogravimetric analysis*

Thermogravimetric experiments were performed using a German NETZSCH TG209F1 analyser. The heating rate was 20 °C/min, starting at 25 °C and reaching 1000 °C. Throughout the experiment, the atmosphere was ambient air, with an air intake rate of 60 ml/min. The thermodynamic curves of the sludge, cotton straw, and corn stover were analysed in individually and in combinations of sludge with corn stover or cotton straw<sup>19,20</sup>. Table 2 shows the technical parameters of thermogravimetric analyzer.

#### *Kinetic analysis*

Activation energy is the energy required for a substance to change from its normal state to an active state; the higher the activation energy, the more difficult it is for a substance to react chemically<sup>21</sup>. In this experiment, the Coats-Redfern<sup>22,23</sup> model was used to calculate the activation energy of an inhomogeneous system under non-isothermal conditions, using Eqs. 1 and 2:

$$\frac{d\alpha}{dT} = \frac{A}{\beta} \exp\left(-\frac{E}{RT}\right) f(\alpha) \quad (1)$$

$$\alpha = \frac{m_0 - m_t}{m_0 - m_\infty} \quad (2)$$

| Name     | Type                  | Place of origin |
|----------|-----------------------|-----------------|
| SHCL-800 | Sulfur analyzer       | China           |
| SDCHN536 | CHN analyzer          | China           |
| HYHW-8A  | Automatic calorimeter | China           |
| TQ-3     | CH analyzer           | China           |

**Table 1.** Instrument type and model.

| TG209F1                             |   |
|-------------------------------------|---|
| Type                                | TG209F1                                     |
| Brand                               | NETZSCH                                     |
| Place of origin                     | Germany                                     |
| Measuring range                     | 10–1100°C                                   |
| Rate of heating and rate of cooling | 0.001–200 K/min                             |
| Weighing range                      | 2000 mg                                     |
| Atmosphere                          | Inert, oxidizing, reducing, static, dynamic |

**Table 2.** Thermogravimetric analyzer (TG/DTG) technical parameters.

where  $A$  is the prime factor;  $\beta$  is the rate of temperature increase, °C/min;  $E$  is the activation energy, kJ/mol;  $R$  is the ideal gas constant, 8.314 J/mol-K;  $T$  is the thermodynamic temperature, K;  $\alpha$  is the percent conversion;  $m_0$  is the initial mass of the sample, mg;  $m_\infty$  is the sample reaction termination mass, mg;  $m_t$  is the sample mass at time  $t$ , mg;  $f(\alpha)$  is the mechanism function; and  $G(\alpha)$  is the kinetic model function.

Through integration of Eq. (1), we get Eq. (3),

$$\int_0^\alpha \frac{d\alpha}{f(\alpha)} = \frac{A}{\beta} \int_{T_0}^T \exp\left(-\frac{E}{RT}\right) dT \quad (3)$$

where  $G(\alpha) = \int_0^\alpha \frac{d\alpha}{f(\alpha)}$ . Using the Coats-Redfern model, the integral of Eq. (3) takes the logarithmic form, as expressed in Eq. (4):

$$\ln\left[\frac{G(\alpha)}{T^2}\right] = \ln\left(\frac{AR}{\beta E}\right) - \frac{E}{RT} \quad (4)$$

where  $1/T$  represents the horizontal axis and  $\ln(G(\alpha)/T^2)$  represents the vertical axis. The function was linearly fit to find the activation energy, and pre-exponential factor  $A$ .

#### Simulation analysis

In this study, a 330 MW quadrangular tangent circle commonly used in Xinjiang is used for numerical simulation. The diameter, width, and height of the boiler were 12.80 m, 12.80 m, and 55.23 m, respectively. The operating parameters of the boiler are listed in Table 3 and the simulated combustion feed ratios are listed in Table 4.

In this study, Fluent 14.0 from Ansys software was used, which consists of 565,206 structural units, as shown in Fig. 3. The grid was refined at important locations, such as primary air nozzles and material nozzles. The modelling and computational methods considered for the validity and accuracy of the model were as follows:

| Name  | Primary wind speed (m/s) | Primary air temperature (°C) | Secondary wind speed (m/s) | Secondary air temperature (°C) | Burn-out wind speed (m/s) | Burnout wind temperature (°C) | Inlet temperature (°C) | Mean static pressure (Pa) | Wall temperature (°C) | Grain size (mm) |
|-------|--------------------------|------------------------------|----------------------------|--------------------------------|---------------------------|-------------------------------|------------------------|---------------------------|-----------------------|-----------------|
| Value | 27                       | 69.85                        | 46                         | 360.85                         | 46                        | 360.85                        | 69.85                  | -80                       | 926.85                | 0.075~0.6       |

**Table 3.** Operational parameters of the 330MW quad-cut circle combustion furnace setup.

| working condition | Sludge (%) | Cotton straw (%) | Corn stover (%) |
|-------------------|------------|------------------|-----------------|
| 1                 | 100        | 0                | 0               |
| 2                 | 90         | 10               | 0               |
| 3                 | 80         | 20               | 0               |
| 4                 | 70         | 30               | 0               |
| 5                 | 60         | 40               | 0               |
| 6                 | 50         | 50               | 0               |
| 7                 | 90         | 0                | 10              |
| 8                 | 80         | 0                | 20              |
| 9                 | 70         | 0                | 30              |
| 10                | 60         | 0                | 40              |
| 11                | 50         | 0                | 50              |

**Table 4.** Simulated combustion feed ratios of sludge, cotton straw, and corn stover for a 330 MW quad-circular combustion furnace.

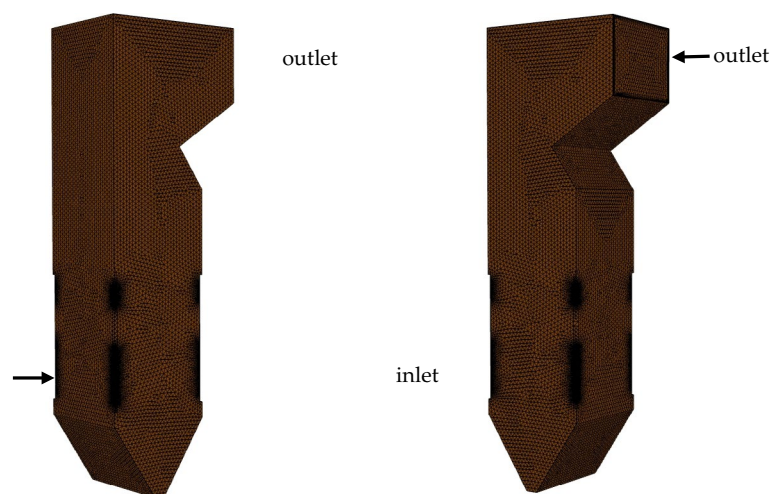


**Figure 3.** Modelling and meshing of a four-corner, cut-circle combustion furnace.

1. Standard modelling equations including the conservation of mass, conservation of energy, conservation of momentum, and conservation of substance concentration equations were used<sup>24</sup>.
2. A matter transport model was combined with a discrete-phase model to simulate boiler combustion<sup>25</sup>.
3. A simulation of turbulent gas flow in pulverised coal boilers was carried out using the standard j-e turbulence model<sup>26</sup>.
4. Radiative heat transfer was calculated using the P-1 radiation model, because heat transfer affects combustion and particle behaviour<sup>27</sup>.
5. The surface reaction of the fuel combustion was modelled using a finite rate/vortex dissipation model<sup>28</sup>.
6. The  $\text{NO}_x$  model primarily considered thermal  $\text{NO}_x$  and fuel  $\text{NO}_x$ <sup>29,30</sup>.

## Results and discussion

### Elemental analysis and industrial analysis

The experiments were carried out according to the experimental methods in “Elemental and industrial analyses and calorific values” and the results are shown in Table 5. The C and H contents of the sludge were lower than those of the cotton straw or corn stover, while the contents of O, N, and S were higher than those of the cotton straw or corn stover. Generally, greater amounts of C correlate with greater heat generation, while high H content makes ignition and burning easier. However, higher O contents can inhibit combustion<sup>31</sup>. Therefore, cotton straw or corn stover has a higher heat generation during combustion than sludge, and ignition and combustion are easier than sludge. The industrial analysis showed that the sludge moisture and ash contents were higher than those of cotton straw and corn stover, but the volatile fraction and fixed carbon ratios were lower. Lower moisture and ash contents reduce energy consumption<sup>32,33</sup>, thereby improving the thermal efficiency of combustion; meanwhile, higher volatile matter and fixed carbon ratios, generate more heat during combustion, improving the utilisation rate of combustion. This result suggests that cotton straw and corn stover require less energy consumption during combustion and maintain higher thermal efficiency and heat generation than does sludge alone.

### Microstructure analysis

The SEM images of the sludge, cotton straw, and corn stover before and after blending are shown in Fig. 4. As shown in Fig. 4a, the sludge consisted of irregularly sized particles with rough surfaces, complex lumpy structures, and pores of different sizes. As shown in Fig. 4b, cotton straw had a laminar void and a relatively loose structure. As shown in Fig. 4c, corn stover also had a lamellar structure, but with a denser outer surface. As shown in Fig. 4d,e, cotton straw and corn stover particles were attached to the surface of the sludge particles after blending.

| Sample       | Elemental analysis (%) |           |           |           |           | Industrial analysis (%) |          |          |           | $Q_{net,d}$ (MJ/kg) |
|--------------|------------------------|-----------|-----------|-----------|-----------|-------------------------|----------|----------|-----------|---------------------|
|              | $C_{daf}$              | $H_{daf}$ | $O_{daf}$ | $N_{daf}$ | $S_{daf}$ | $M_{ad}$                | $A_{ad}$ | $V_{ad}$ | $FC_{ad}$ |                     |
| Sludge       | 32.84                  | 3.86      | 57.53     | 5.06      | 0.71      | 19.68                   | 30.52    | 43.34    | 6.46      | 11.05               |
| Cotton straw | 48.70                  | 6.05      | 44.67     | 0.47      | 0.11      | 5.86                    | 5.12     | 70.21    | 18.81     | 16.94               |
| Corn stover  | 50.26                  | 6.20      | 42.36     | 1.00      | 0.18      | 6.62                    | 6.02     | 67.04    | 20.32     | 16.80               |

**Table 5.** Elemental analyses, industrial analyses, and calorific values of sludge, cotton straw, and corn stover.



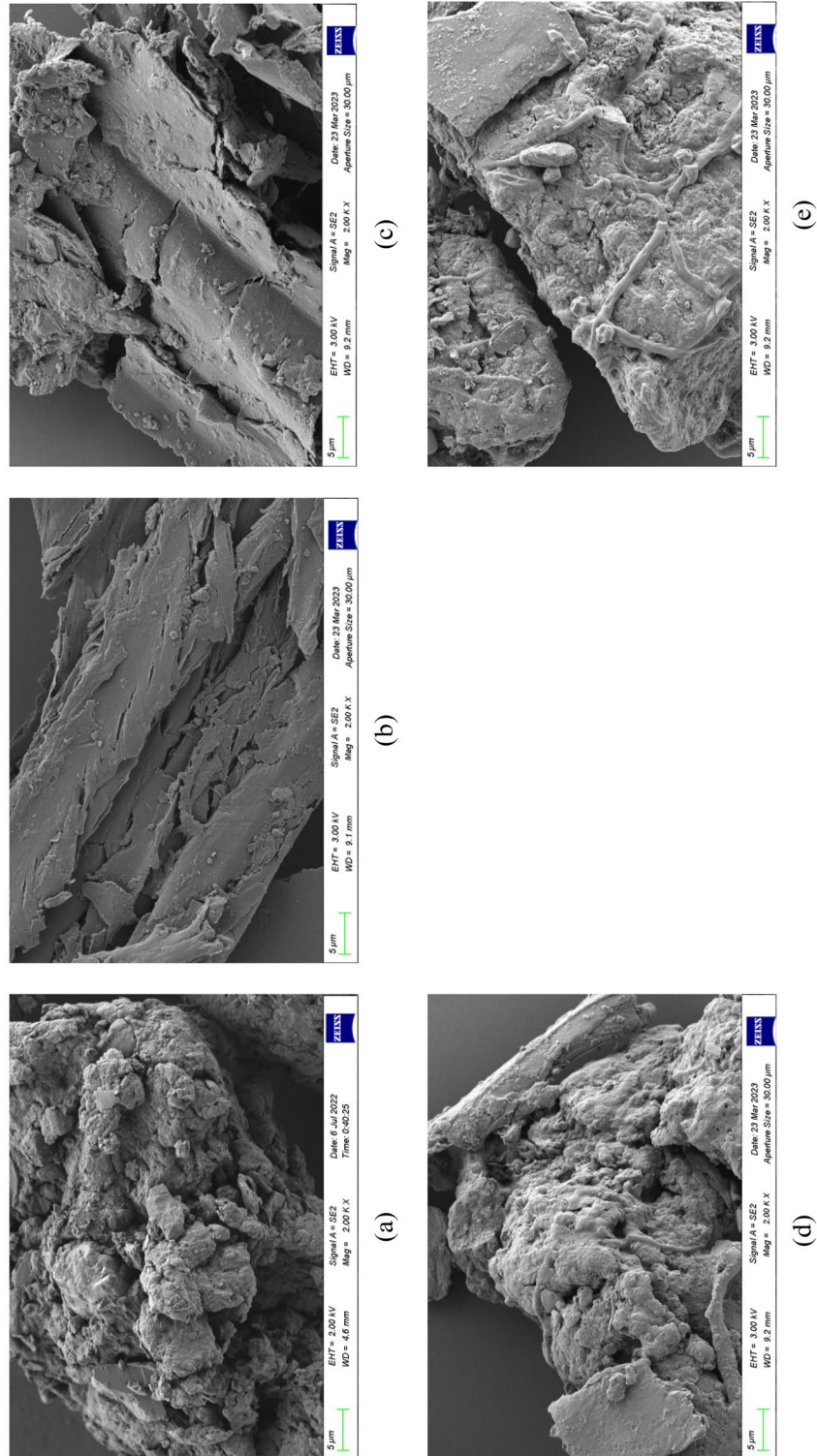


**Figure 4.** Scanning electron micrographs of the microstructures of sludge, cotton straw, and corn stover before and after blending. **(a)** Cotton straw; **(b)** Sludge; **(c)** Corn stover; **(d)** Sludge + cotton straw; **(e)** Sludge + corn stover.

### Thermogravimetric analysis

Relevant data show that when sludge and other substances are mixed and burned, the water content is reduced to 30–40%<sup>34</sup>, which is conducive to increasing the temperature of combustion, and the combustion is more stable<sup>25</sup>. So this study selected 60% sludge and 40% cotton straw for mixing combustion, thermogravimetric experiment results are shown in Fig. 5a. The weight loss stages of the sludge were the same as those of cotton straw and corn stover across all three stages<sup>35</sup>; however, the maximum rate of weight loss and final weight loss rate in the three stages of cotton straw and corn stover was greater than that of the sludge, indicating that the combustion of cotton straw and corn stover was more complete, and the burning rate was higher than that of sludge alone<sup>36</sup>.

Figure 5b shows the thermogravimetric curves of the sludges mixed with cotton straw or corn stover. The TG-DTG of both sets of mixed samples showed three phases, each of which occurred at approximately the same temperature interval as in the case of sludge burning alone, indicating that mixing sludge burning with these two types of agricultural waste did not alter the weight loss phase. The blended combustion increased the weight loss rate across the three stages, but the weight loss rate of the 60% sludge + 40% cotton straw was greater<sup>37</sup> than that of the 60% sludge + 40% corn stover ratio, and the blended combustion left less residue, suggesting that the addition of the agricultural waste effectively improved the sludge combustion rate, made the sludge burn more fully, and resulted in a higher burnout rate<sup>38</sup>.

### Non-isothermal kinetic fitting and activation energy study

The results of non-isothermal kinetic fitting are shown in Fig. 6 and the results of the activation energy calculations are shown in Table 6. The average activation energy of sludge alone was 116.65 kJ/mol, and the addition of cotton straw or corn stover reduced the activation energy of sludge by 12.74 kJ/mol for the 60% sludge + 40% cotton straw mixture and 5.58 kJ/mol for the 60% sludge + 40% corn stover mixture. Therefore, the addition of cotton straw or corn stover promoted sludge combustion<sup>39</sup>, though the cotton straw mix had a stronger positive effect. Taken together, these results suggest that the mixture of 60% sludge + 40% cotton straw produced the lowest reaction activation energy of sludge combustion, and thus exhibited better combustion performance<sup>40,41</sup>.

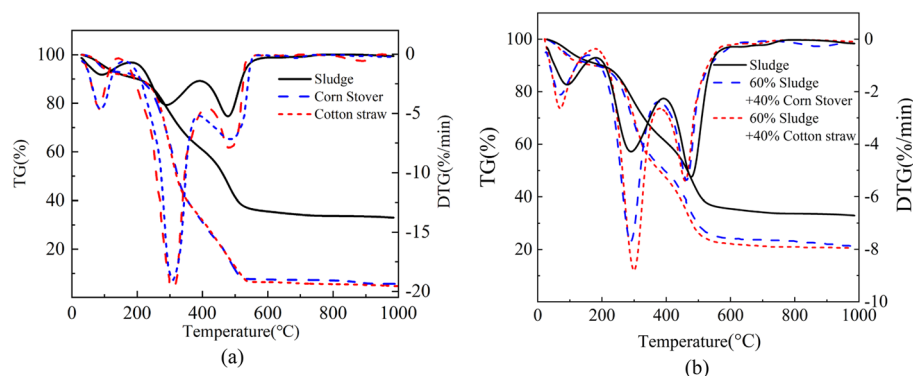


**Figure 5.** Thermogravimetric curves. (a) Thermogravimetric curves of sludge, cotton straw, and corn stover burned individually; (b) thermogravimetric curve of combustion of sludge blended with cotton straw and corn stover.

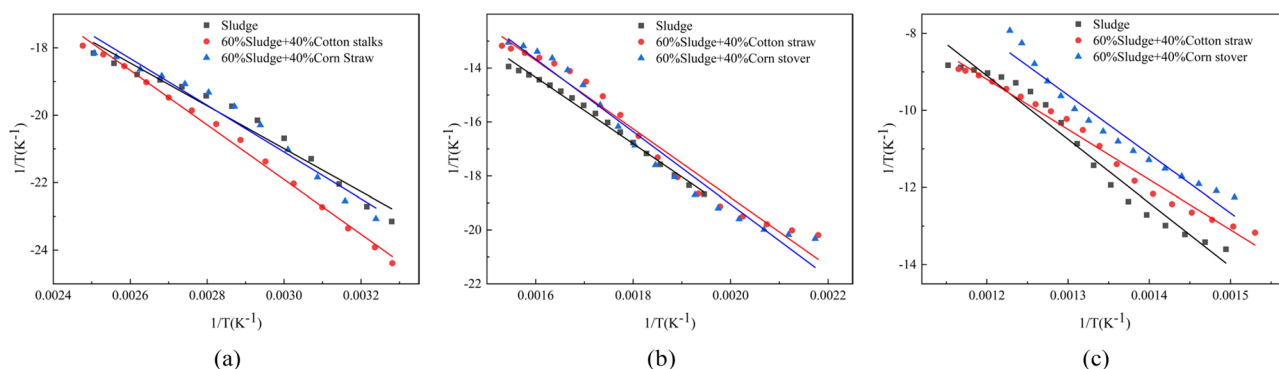


**Figure 6.** Kinetic fitting of sludge, cotton straw and corn stover combustion alone and blended combustion. (a) The first stage; (b) The second stage; (c) The third stage.

| Materialistic                 | Stage | Activation energy $E$ (kJ/mol) | Average activation energy $E_m$ (kJ/mol) | Indexing factor $A$ ( $\text{min}^{-1}$ ) | Percentage weight loss $f$ (%) |
|-------------------------------|-------|--------------------------------|--|---|--------------------------------|
| Sludge                        | 1     | 67.36                          | 116.65                                   | $1.79 \times 10^3$                        | 9.53                           |
|                               | 2     | 103.14                         |  | $6.23 \times 10^4$                        | 24.19                          |
|                               | 3     | 141.30                         |  | $2.89 \times 10^7$                        | 32.31                          |
| 60% Sludge + 40% Cotton straw | 1     | 52.85                          | 103.91                                   | $1.86 \times 10$                          | 8.83                           |
|                               | 2     | 109.55                         |  | $4.55 \times 10^3$                        | 49.27                          |
|                               | 3     | 110.98                         |  | $2.56 \times 10^5$                        | 24.44                          |
| 60% Sludge + 40% Corn Stover  | 1     | 57.68                          | 111.07                                   | $1.58 \times 10^2$                        | 8.89                           |
|                               | 2     | 111.93                         |  | $1.06 \times 10^6$                        | 45.44                          |
|                               | 3     | 127.13                         |  | $1.33 \times 10^7$                        | 27.11                          |

**Table 6.** Elemental analyses, industrial analyses, and calorific values of sludge, cotton straw, and corn stover.

## Numerical simulation of boiler combustion

### *Temperature cloud of sludge mixed with cotton straw combustion*

The variations in boiler temperature for the combustion of sludge and cotton straw at different blending ratios are shown in Fig. 7. Temperature cloud of sludge and cotton straw combustion at different blending ratios. (a) Sludge; (b) 90% sludge + 10% cotton straw; (c) 80% sludge + 20% cotton straw; (d) 70% sludge + 30% cotton straw; (e) 60% sludge + 40% cotton straw; (f) 60% sludge + 40% cotton straw. The six groups of hearth temperature cloud maps were ultimately similar in distribution, and the temperature fields were all relatively stable, indicating that the addition of cotton straw did not affect the flame combustion pattern in the hearth. With an increase in the cotton straw blending ratio, however, the furnace chamber temperature gradually increased. The highest temperature of sludge combustion alone was 1485.60 °C, while the maximum temperature was 1564.12 °C after adding 50% cotton straw, likely because the addition of cotton straw increased the fixed carbon content and reduced the moisture and ash contents of the sludge, resulting in a higher combustion temperature in the furnace.

### *Temperature cloud of sludge mixed with corn stover combustion*

The boiler temperature variations of the sludge and corn stover combustion at different blending ratios are shown in Fig. 8.

The simulation results for the combustion of the sludge and corn stover blends appear similar to those for the sludge and cotton straw blends, with the furnace chamber temperature increasing with the increase in corn stover content. When the proportion of corn stover was 50% sludge to 50% corn stover, the highest temperature, 1547.92 °C, was reached, likely because the addition of corn stover reduced the moisture and ash contents of the sludge and increased the fixed carbon content, thereby increasing the combustion temperature of the furnace.

### *Pollutant emissions from co-combustion of sludge and cotton straw*

Figure 9 shows the temperature and pollutant emission profiles of sludge and cotton straw combustion under different blending ratios. Based on the temperature curves, the overall trend of the six sets of curves was similar, with the temperature first increasing and then slowly decreasing as the height of the hearth increases<sup>42</sup>. The high-temperature region of furnace combustion occurred in the main combustion region, which is consistent with actual boiler operation<sup>43</sup>. As the proportion of cotton straw increased, the combustion temperature in the furnace chamber also gradually increased.

The CO mass fraction curve with hearth height first increased and then decreased. CO mass fraction increased with the increase of cotton straw blending ratio, the sludge combustion alone for  $8.42 \times 10^{-5}$ , blended with 50% cotton straw for  $6.47 \times 10^{-4}$ , indicating that greater levels of cotton straw during combustion increased the production of CO. This is because the temperature of the chamber increases more rapidly for a larger proportion of cotton straw; thus, the mixture burns faster and the surrounding oxygen is consumed at a faster rate than the incoming oxygen, resulting in insufficient local burning and an increase in the mass fraction of CO<sup>44</sup>.

SO<sub>2</sub> production appeared to increase and then decrease with the increase in furnace height; in the main combustion zone, the sludge combustion of the SO<sub>2</sub> mass fraction was the largest,  $2.10 \times 10^{-3}$ . The SO<sub>2</sub> mass fraction peaks reduced significantly with a larger fraction of cotton straw; specifically, blending with 50% cotton straw resulted in the lowest production of SO<sub>2</sub>. The formation of SO<sub>2</sub> is closely related to the sulfur content of the material. The content of elemental S in sludge was higher than that of cotton straw, therefore, with an increase in the cotton straw blending ratio, the content of elemental S decreased, and the emission of SO<sub>2</sub> decreased.

The NO concentration increased and then decreased along the hearth height, with a slight increase near the flue gas outlet. The NO concentration was mainly concentrated near the main combustion zone, which had the highest temperature and produced large amounts of fuel- and thermal-type NO<sub>x</sub><sup>45</sup>. Lower temperatures in the lower and upper parts of the boiler reduce thermal NO<sub>x</sub> production. There was a slight increase in the NO concentration near the furnace exit, likely due to the increase in NO emissions resulting from poorer combustion performance. As the percentage of cotton straw increased, the concentration of NO decreased gradually, while the highest value of NO concentration for sludge combustion alone was 794.42 mg/m<sup>3</sup>, and 586.41 mg/m<sup>3</sup> after blending with 50% cotton straw, which resulted in a decrease of 208.01 mg/m<sup>3</sup>.



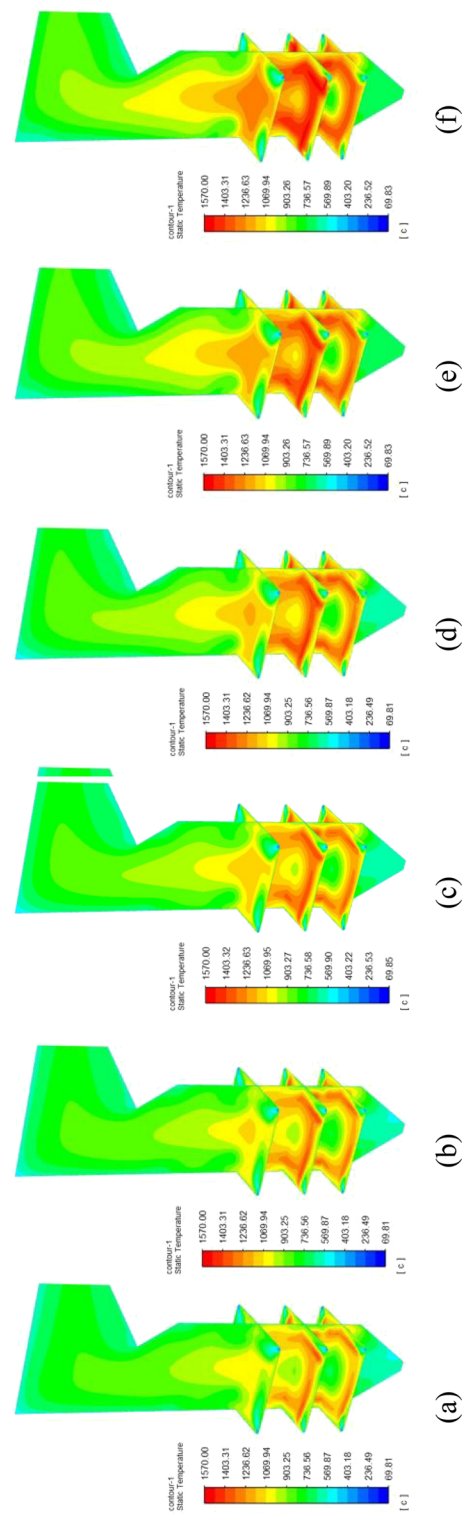


**Figure 7.** Temperature cloud of sludge and cotton straw combustion at different blending ratios. (a) Sludge; (b) 90% sludge + 10% cotton straw; (c) 80% sludge + 20% cotton straw; (d) 70% sludge + 30% cotton straw; (e) 60% sludge + 40% cotton straw; (f) 60% sludge + 40% cotton straw.

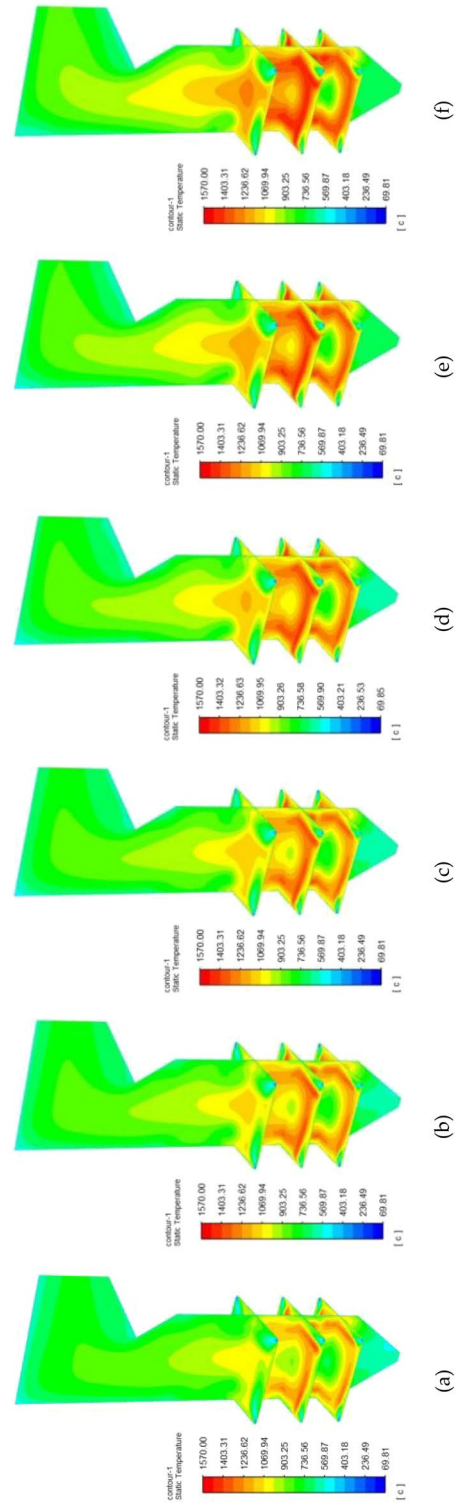


**Figure 8.** Temperature cloud of sludge and corn stover combustion at different blending ratios. (a) Sludge; (b) 90% Sludge + 10% Corn stover; (c) 80% sludge + 20% corn stover; (d) 70% sludge + 30% corn stover; (e) 60% sludge + 40% corn stover; (f) 50% sludge + 50% corn stover.

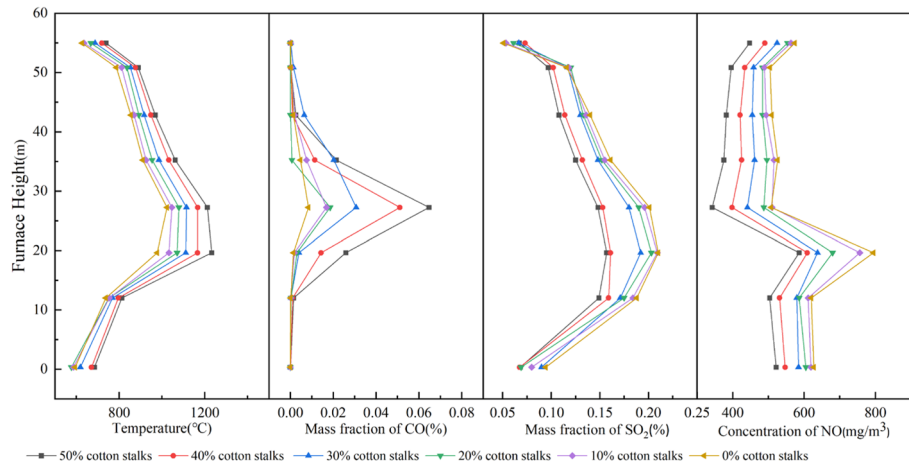


**Figure 9.** Temperature and pollutant emission distribution of sludge and cotton straw combustion at different blending ratios.

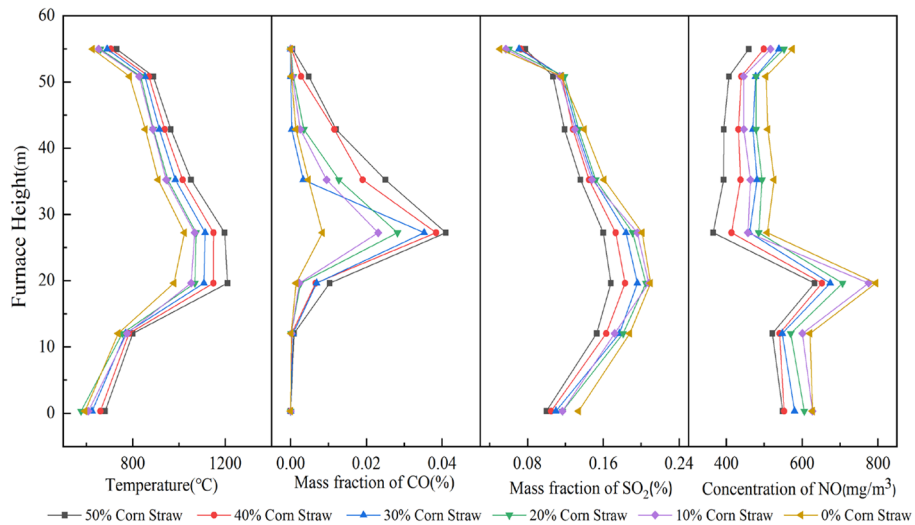
*Pollutant emissions from combustion of sludge with corn stover*

Figure 10 shows the temperature and pollutant emission profiles of sludge and corn stover combustion for different blending ratios. With an increase in the height of the furnace chamber, the temperature first rose and then slowly decreased, and the temperature inside the furnace chamber gradually increased as the proportion of corn stover increased in the blend.

The CO mass-fraction profile peaked in the main combustion zone and approached zero near the slag and smoke outlets. The maximum CO mass fraction was  $4.1 \times 10^{-4}$  for the with 50% corn stover blend. The higher the corn stover proportion in the blend, the higher the resulting CO mass fraction.

The SO<sub>2</sub> trend was similar to that of the boiler combustion temperature, with high SO<sub>2</sub> content in the high-temperature zone and low SO<sub>2</sub> content in the lower part of the furnace and exhaust port. As the proportion of corn stover increased, the SO<sub>2</sub> in the furnace chamber gradually decreased. The mass fraction of SO<sub>2</sub> was  $1.68 \times 10^{-3}$  when mixed with 50% corn stover.

The NO concentration curve first increased then decreased, with the curve flattening at approximately 30 ~ 50 m furnace height followed by a slight increase at the flue gas outlet. The lowest NO concentration, 632.61 mg/m<sup>3</sup>, was produced from the 50% corn stover blend, and the NO concentration at the furnace exit also decreased with increasing corn stover blending ratio. This is consistent with the findings of Hongpeng Liu<sup>46</sup> et al. (2021) that the incorporation of corn stover reduces NO and SO<sub>2</sub> emissions.



**Figure 10.** Temperature and pollutant emission distribution of sludge and corn stover combustion at different blending ratios.

### Comparative analysis of sludge blended with different ratios of cotton straw and corn stover for combustion

A comparison of the simulation results for the combustion of sludge blended with cotton straw or corn stover is shown in Fig. 11. Figure 11a shows that, with an increase in the proportion of cotton straw or corn stover, the combustion temperature in the furnace chamber gradually increased, with the greatest increase coming from the cotton straw mix. For the 50% cotton straw or corn stover sludge mixes, the temperatures increased by 226.24 °C and 173.65 °C, respectively.

The combustion of sludge mixed with either cotton straw or corn stover resulted in increased CO emissions. When the proportion of cotton straw or corn stover in the sludge blend was less than 30%, the amount of CO produced by the cotton straw blend was lower, whereas when the mixing amount of cotton straw or corn stover was 30%–50%, the amount of CO produced by the mixed combustion of sludge and corn stover was smaller.

Overall, the combustion of sludge mixed with cotton straw or corn stover reduced SO<sub>2</sub> and NO emissions, which is due to the fact that SO<sub>2</sub> and NO emissions are mainly determined by the sulphur and nitrogen content of the substance<sup>47</sup>. The elemental analysis shows that, under the same blending ratio, lower SO<sub>2</sub> emissions from combustion of sludge mixed with cotton straw occurred due to lower elemental S in cotton straw. Moreover, NO is mainly composed of fuel and thermal types<sup>48</sup>, of which fuel types account for 60%–80% of all NO, and thermal types account for about 20%. Fuel-type NO content is mainly determined by the N-element content of the burning material. Mao Ya<sup>49</sup> et al. (2017) found that the NO burned by cotton straw was lower than that of corn stover. Thus, given that cotton straw had only half the N content of corn stover<sup>50</sup>, the NO produced by blending cotton straw burning was lower than that of corn stover.

## Conclusions

1. Blending sludge with cotton straw or corn stover for combustion increased the rate of weight loss and combustion exhaustion and decreased the activation energy of the reaction. When a ratio of 60% of sludge to 40% of cotton straw was burned, the activation energy decreased by 12.74 kJ/mol, while that with corn stover

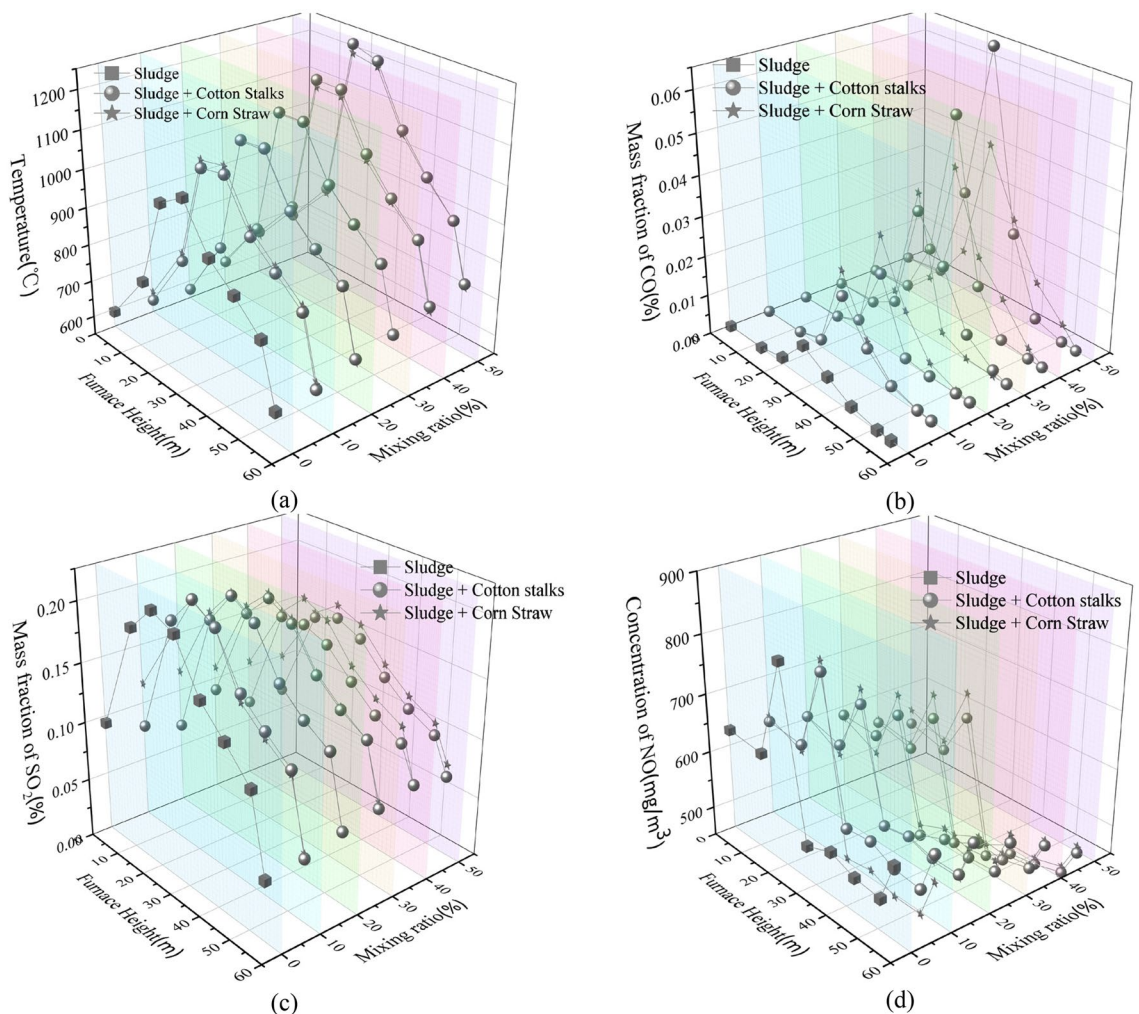


**Figure 11.** Comparison of combustion simulation results of sludge blended with cotton straw or corn stover. (a) Temperature; (b) CO mass fractions; (c) of mass fractions of SO<sub>2</sub>; (d) NO concentrations.



- decreased by 5.58 kJ/mol. In summary, the addition of cotton straw or corn stover improved combustion performance compared to that of sludge alone.
- At the same blending ratio, the combustion temperatures of sludge and cotton straw were higher than those of sludge and corn stover. Specifically, the furnace temperature increased by 226.24 and 173.65°C when the percentages of cotton straw and corn stover, respectively, were 50%.
  - The CO content in the boiler increased with increasing cotton straw or corn stover blending ratios. When the ratio of cotton straw or corn stover was less than 30%, the CO content of the sludge and cotton straw blending and combustion was smaller. When the ratio of cotton straw to corn stover was 30%-50%, the CO content of the sludge and corn stover blending and combustion was smaller.
  - The SO<sub>2</sub> and NO contents in the boiler gradually decreased with an increase in the blending ratio of cotton straw or corn stover. Because the S and N contents of the cotton straw were lower than those of the corn stover, the SO<sub>2</sub> and NO contents produced by the mixed burning of sludge and cotton straw were lower than those of sludge and corn stover at the same ratio.

Experimental studies and finite element simulations have shown that mixing sludge and cotton straw for combustion can be more efficient in reducing the activation energy required for combustion, increasing the temperature of blended combustion, and reducing the emission of pollutants from blended combustion, compared to blending with corn stover. Therefore, a more in-depth study on sludge and cotton-straw-blended combustion should be carried out to further optimise the blending method and combustion conditions to improve the performance of sludge combustion in accordance with the Dual Carbon Strategy goals.

### Data availability

The dataset used and analysed during the current study are available from the corresponding author (Jing Li) on reasonable request.

Received: 26 December 2023; Accepted: 12 March 2024

Published online: 15 March 2024

### References

- Jaworski, T. J. & Kajda-Szcześniak, M. Study on the similarity of the parameters of biomass and solid waste fuel combustion for the needs of thermal power engineering. *Sustainability* **12**, 7894 (2020).
- Syed-Hassan, S. S. A., Wang, Y., Hu, S., Su, S. & Xiang, J. Thermochemical processing of sewage sludge to energy and fuel: fundamentals, challenges and considerations. *Renew. Sustain. Energy Rev.* **80**, 888–913 (2017).
- Commission, N. D. A. R. & Development, M. O. H. A. Implementation Program of Mending Shortcomings and Strengthening Weaknesses of Urban Living Sewage Treatment Facilities. [https://www.gov.cn/zhengce/zhengceku/2020-08/06/content\\_5532768.htm](https://www.gov.cn/zhengce/zhengceku/2020-08/06/content_5532768.htm). (2020).
- Zhou, Y., Li, F., Xin, Q., Li, Y. & Lin, Z. Historical variability of cotton yield and response to climate and agronomic management in Xinjiang, China. *Sci. Total Environ.* **912**, 169327 (2024).
- Ong, H. C. et al. A state-of-the-art review on thermochemical conversion of biomass for biofuel production: a tg-ftir approach. *Energy Conv. Manag.* **209** (2020).
- Sidi-Yacoub, B., Oudghiri, F., Belkadi, M. & Rodríguez-Barroso, R. Characterization of lignocellulosic components in exhausted sugar beet pulp waste by tg-ftir analysis. *J. Therm. Anal. Calorim.* **138**, 1801–1809 (2019).
- Shi, Y. et al. Effects of biomass blending on combustion performance of sewage sludge. *China Environ. Sci.* **42**, 3796–3803 (2022).
- Baek, G. et al. Combustion of the pellets of sewage sludge and woody biomass blend in a circulating fluidized bed combustor: effect of oxidant conditions on the reduction of pollutant emissions. *J. Korean Soc. Combust.* **25**, 37–47 (2020).
- Wang, Y., Liu, Y., Yang, W., Zhao, Q. & Dai, Y. Evaluation of combustion properties and pollutant emission characteristics of blends of sewage sludge and biomass. *Sci. Total Environ.* **720**, 137365–137373 (2020).
- Liu, J. et al. (Co-)Combustion of additives, water hyacinth and sewage sludge: Thermogravimetric, kinetic, gas and thermodynamic modeling analyses. *Waste Manag.* **81**, 211–219 (2018).
- Sung, J. et al. Oxy-fuel co-combustion of sewage sludge and wood pellets with flue gas recirculation in a circulating fluidized bed. *Fuel Process. Technol.* **172**, 79–85 (2018).
- Bagheri, M., Öhman, M. & Wetterlund, E. Techno-economic analysis of scenarios on energy and phosphorus recovery from mono- and co-combustion of municipal sewage sludge. *Sustainability* **14**, 2603 (2022).
- Ni, Z. et al. Investigation of co-combustion of sewage sludge and coffee industry residue by tg-ftir and machine learning methods. *Fuel* **309**, 122082 (2022).
- Xu, G. et al. Investigation of the so<sub>2</sub> release characteristics during co-combustion of fenton/cao treated municipal sewage sludge and rice husk. *J. Environ. Chem. Eng.* **10**, 108475 (2022).
- Fu, P. et al. Ftir study of pyrolysis products evolving from typical agricultural residues. *J. Anal. Appl. Pyrolysis.* **88**, 117–123 (2010).
- Li, T., Song, F., Wu, F., Huang, X. & Bai, Y. Heterogeneous dynamic behavior and synergetic evolution mechanism of internal components and released gases during the pyrolysis of aquatic biomass. *Environ. Sci. Technol.* **56**, 13595–13606 (2022).
- Zong, P. et al. Pyrolysis behavior and product distributions of biomass six group components: starch, cellulose, hemicellulose, lignin, protein and oil. *Energy Conv. Manag.* **216**, 112777 (2020).
- Cao, H. et al. Computational fluid dynamics simulation of combustion and selective non-catalytic reduction in a 750 T/D waste incinerator. *Processes* **11** (2023).
- Magdziarz, A. & Wilk, M. Thermogravimetric study of biomass, sewage sludge and coal combustion. *Energy Conv. Manag.* **75**, 425–430 (2013).
- Park, J. M., Keel, S., Yun, J., Yun, J. H. & Lee, S. Thermogravimetric study for the co-combustion of coal and dried sewage sludge. *Korean J. Chem. Eng.* **34**, 2204–2210 (2017).
- Xu, T., Wang, C., Hong, D., Li, S. & Yue, S. The synergistic effect during co-combustion of municipal sludge and coal: Experimental and reaxff molecular dynamic study. *Energy* **262** (2023).
- Chen, Y., Gui, H., Xia, Z., Chen, X. & Zheng, L. Thermochemical and toxic element behavior during co-combustion of coal and municipal sludge. *Molecules* **26**, 4170 (2021).
- Bi, H. et al. Pyrolysis characteristics, artificial neural network modeling and environmental impact of coal gangue and biomass by tg-ftir. *Sci. Total Environ.* **751**, 142293 (2021).



24. Qi, X., Ma, X., Yu, Z., Huang, Z. & Teng, W. Numerical simulation of municipal waste and food digestate blending combustion and nox reduction under oxygen-enriched atmospheres. *Fuel*. **345**, 128115 (2023).
25. Lin, T., Liao, Y., Dai, T. & Ma, X. Investigation on co-disposal technology of sludge and municipal solid waste based on numerical simulation. *Fuel*. **343**, 127882 (2023).
26. Al-Abbas, A. H., Naser, J. & Dodds, D. Cfd modelling of air-fired and oxy-fuel combustion in a large-scale furnace at loy yang a brown coal power station. *Fuel*. **102**, 646–665 (2012).
27. Li, J., Brzdekiewicz, A., Yang, W. & Blasiak, W. Co-firing based on biomass torrefaction in a pulverized coal boiler with aim of 100% fuel switching. *Appl. Energy*. **99**, 344–354 (2012).
28. Lin, T., Liao, Y., Yang, X. & Ma, X. Numerical simulation analysis on the characteristics of municipal domestic waste with high calorific value and sludge co-combustion. *Energy Sources. A. Recovery Utilization Environ. Effects*. 1–15 (2021) (ahead-of-print).
29. Li, K., Thompson, S. & Peng, J. X. Modelling and prediction of Nox emission in a coal-fired power generation plant. *Control Eng. Practice*. **12**, 707–723 (2004).
30. Hill, S. C. & Smoot, L. D. Modeling of nitrogen oxides formation and destruction in combustion systems. *Prog. Energy Combust. Sci*. **26**, 417–458 (2000).
31. Ma, M. *et al.* Gas emission characteristics of sewage sludge co-combustion with coal: Effect of oxygen atmosphere and feedstock mixing ratio. *Fuel*. **322**, 124102 (2022).
32. Lin, B., Zhou, J., Qin, Q., Song, X. & Luo, Z. Thermal behavior and gas evolution characteristics during co-pyrolysis of lignocellulosic biomass and coal: a tg-ftir investigation. *J. Anal. Appl. Pyrolysis*. **144**, 104718 (2019).
33. Volli, V. *et al.* Thermal degradation behaviour, kinetics, and thermodynamics of bombax malabarica seeds through Tg-Ftir and Py-Gc/Ms analysis. *Sustain. Energy Technol. Assess.* **57**, 103150 (2023).
34. Liang, D., Li, Y. & Zhou, Z. Numerical study of thermochemistry and trace element behavior during the co-combustion of coal and sludge in boiler. *Energies*. **15**, 888 (2022).
35. Li, Y. *et al.* Synergistic effect of combined hydrothermal carbonization of fenton's reagent and biomass enhances the adsorption and combustion characteristics of sludge towards eco-friendly and efficient sludge treatment. *Sci. Total Environ.* **825** (2022).
36. Liu, R., Liu, G., Yousaf, B., Niu, Z. & Abbas, Q. Novel investigation of pyrolysis mechanisms and kinetics for functional groups in biomass matrix. *Renew. Sust. Energ. Rev.* **153**, 111761 (2022).
37. Wilk, M., Magdziarz, A., Jayaraman, K., Szymańska-Chargot, M. & Gökalp, I. Hydrothermal carbonization characteristics of sewage sludge and lignocellulosic biomass. A comparative study. *Biomass Bioenergy*. **120**, 166–175 (2019).
38. Chen, J. *et al.* The mixture of sewage sludge and biomass waste as solid biofuels: Process characteristic and environmental implication. *Renew. Energy*. **139**, 707–717 (2019).
39. Wang, C. *et al.* The thermal behavior and kinetics of co-combustion between sewage sludge and wheat straw. *Fuel Process. Technol.* **189**, 1–14 (2019).
40. Xu, G. *et al.* Study On characteristics, hydrogen-rich gas, bio-oil production, and process optimization of co-pyrolysis of sewage sludge and wheat straw. *Case Stud. Therm. Eng.* **45**, 102888 (2023).
41. Guo, S. *et al.* Synergistic effects of co-combustion of sewage sludge and corn stalk and the resulting gas emission characteristics. *Iet Renew. Power Gener.* **14**, 1596–1605 (2020).
42. Tan, P. *et al.* Co-firing sludge in a pulverized coal-fired utility boiler: Combustion characteristics and economic impacts. *Energy (Oxford)*. **119**, 392–399 (2017).
43. Wei, D. *et al.* Influence of fuel distribution on co-combustion of sludge and coal in a 660 Mw tangentially fired boiler. *Appl. Therm. Eng.* **227**, 120344 (2023).
44. Wu, W. *et al.* Three-dimensional full-loop numerical simulation of coal and sludge co-combustion in a circulating fluidized bed. *Fuel*. **337**, 127235 (2023).
45. Xu, J. *et al.* Co-combustion of paper sludge in a 750 T/D waste incinerator and effect of sludge moisture content: A simulation study. *Fuel*. **217**, 617–625 (2018).
46. Liu, H. *et al.* Combustion characteristics and typical pollutant emissions of corn stalk blending with municipal sewage sludge. *Environ. Sci. Pollut. Res.* **28**, 9792–9805 (2021).
47. Sharma, A. & Mohanty, B. Non-isothermal Tg/Dtg-ftir kinetic study for devolatilization of dalbergia sissoo wood under nitrogen atmosphere. *J. Therm. Anal. Calorim.* **146**, 865–879 (2021).
48. Tan, P., Ma, L., Fang, Q., Zhang, C. & Chen, G. Application of different combustion models for simulating the co-combustion of sludge with coal in a 100 Mw tangentially coal-fired utility boiler. *Energy Fuels*. **30**, 1685–1692 (2016).
49. Mao, Y., Jiang, Z., Chen, Z. & Zou, Y. Numerical simulation of combustion of biomass pellets based on fluent. *J. Eng. Thermal Energy Power* **32**, 121–125 (2017).
50. Jeong, Y. *et al.* Investigation and optimization of co-combustion efficiency of food waste biochar and coal. *Sustainability* **15**, 14596 (2023).

## Acknowledgements

This research was funded by the Nature Fund project of the Science and Technology Department of Xinjiang Uygur Autonomous Region, Grant Number 2021D01C074.

## Author contributions

Feng Xu designed the experimental scheme and revised the first draft of the paper. Jing Li and Zihan He conducted experiments and drafted the first manuscript. All authors reviewed the manuscript.

## Competing interests

The authors declare no competing interests.

## Additional information

**Supplementary Information** The online version contains supplementary material available at <https://doi.org/10.1038/s41598-024-56842-4>.

**Correspondence** and requests for materials should be addressed to J.L.

**Reprints and permissions information** is available at [www.nature.com/reprints](http://www.nature.com/reprints).

**Publisher's note** Springer Nature remains neutral with regard to jurisdictional claims in published maps and institutional affiliations.



**Open Access** This article is licensed under a Creative Commons Attribution 4.0 International License, which permits use, sharing, adaptation, distribution and reproduction in any medium or format, as long as you give appropriate credit to the original author(s) and the source, provide a link to the Creative Commons licence, and indicate if changes were made. The images or other third party material in this article are included in the article's Creative Commons licence, unless indicated otherwise in a credit line to the material. If material is not included in the article's Creative Commons licence and your intended use is not permitted by statutory regulation or exceeds the permitted use, you will need to obtain permission directly from the copyright holder. To view a copy of this licence, visit <http://creativecommons.org/licenses/by/4.0/>.

© The Author(s) 2024